IEEE Access
Multidisciplinary | Rapid Review | Open Access Journal

Received November 9, 2018, accepted November 25, 2018, date of publication November 29, 2018,
date of current version December 27, 2018.

Digital Object Identifier 10.1109/ACCESS.2018.2884035

Single Channel Blind Source Separation for Wind Turbine Aeroacoustics Signals Based on Variational Mode Decomposition

YA'NAN ZHANG, SHENGBO QI, AND LIN ZHOU
College of Engineering, Ocean University of China, Tsingtao 266100, China

Corresponding author: Shengbo Qi (qishengbo@ouc.edu.cn)

This work was supported in part by the National Natural Science Foundation of China under Grant 51779237 and in part by the Fundamental Research Funds for the Central Universities under Grant 201861037.

ABSTRACT The acquisition of aeroacoustics signals of wind turbines is of great significance in environmental noise assessment and fault monitoring of blades. The single acoustic sensor is simpler and more flexible than the acoustic sensors array but it lacks spatial analysis capability of the acoustic pressure field, and it is difficult to get pure aeroacoustics signals directly. This paper proposes a single channel blind source separation (SCBSS) method based on variational mode decomposition (VMD) which is applied to the separation of the wind turbine aeroacoustics signals acquired by the single acoustic sensors. The variational mode decomposition of the nonlinear and nonstationary signals based on the data itself completely is adaptive. In addition, the problem of mode mixing and "endpoint effect" has been improved. A novel approach combined correlation criterion with an overall index of orthogonality criterion is proposed in this paper to determine the optimal number of decomposition layers of VMD. We transform single channel underdetermined blind source separation to the non-underdetermined problem by establishing virtual multi-channel signals of the observation signals base on VMD, and separate the signals by joint approximate diagonalization of eigen-matrices (JADE) of fourth-order cumulant matrices. The method proposed in this paper has an excellent separation performance for wind turbine aeroacoustics signals, and the analysis of simulation signals indicates it has a 92.23% average recognition proportion, which is better than BSS based on EMD and EEMD, and the method has an extremely shorter computing time than EEMD-BSS. The analysis of actual signals shows that the suggested method is adaptive and robust for noise.

INDEX TERMS Variational mode decomposition, single channel blind source separation, wind turbine aeroacoustics signals, acquisition of acoustic signals.

I. INTRODUCTION

Wind power industry has a great improvement with the quantity and scale of wind farms increasing and the size of wind turbine becomes greater [1], [2]. The unfavored environmental effects of the wind turbine aeroacoustics noise has gradually been considered [3]. However, there are many unsolved problems in mechanism research field of wind turbine aeroacoustics [4]–[7]. So far, the actual measurement and acquisition by acoustic sensors still an important approach to estimate the level of the wind turbine aeroacoustics noise [8]. Meanwhile, the wind turbine aeroacoustics signals contain the operation condition information of blades, and if fault occurs, the feature of aeroacoustics signals will change correspondingly [9]. Therefore, actual measurement and acquisition of aeroacoustics signals is also important to wind turbine blades condition monitoring.

The acoustic array has a wide range of application in wind turbine aeroacoustics signals measurement and acquisition [10]–[12], but the use of acoustic arrays can be limited by installation space because of complex terrain of onshore wind farms and offshore narrow tower foundations. Considering the practicability of field application, a single acoustic sensor which is more convenient and flexible in use is more suitable. However, disadvantages of the single acoustic sensor are also obvious. Due to the limitation of the number of sensors, a single acoustic sensor does not have the spatial analysis ability of the acoustic pressure field, and the measurement results are often unsatisfactory. At present, there is no relevant

report on the method which is flexible and convenient to use and considers the acoustic acquisition performance as well.

Blind source separation (BSS) is a general method of signal processing and data analysis. It is a process of recovering unknown source signals from observed mixed signals, which has application prospects for wind turbine aeroacoustics signals separation and signal enhancement. Now, the blind source separation has been widely used in speech signal processing [13]–[15], mechanical fault detection [16]–[19] and other fields. Gelle *et al.* [20], [21] proposed a blind source separation method for rotating machine monitoring by assuming the independence of the sources and the linearity of the propagation medium without any prior knowledge of mixing. Roan *et al.* [22] proposed a blind source separation algorithm based on information maximization which was essentially a nonlinear adaptive independent component analysis (ICA) method and applied to gear vibration measurement. McNeill and Zimmerman*et al.* [23] introduced the second-order statistics into blind source separation for mode parameter identification by joint approximate diagonalization (JAD). Yang *et al.* [24] put forward a new blind source separation method based on sparse component analysis (SCA) to solve underdetermined blind source separation problems.

The original acoustic signals contain not only pure aeroacoustics signals, but a large number of complex and changeable environmental background noise signals such as wind noise and mechanical noise signals, as well as the nonlinear coupling signals between aeroacoustics noise and various environmental background noise. In addition, acoustic sensors will introduce transmission noise in the process of acquisition and processing inevitably. The statistical features of the acquired signals are time related and non-stationary. At the same time, the signals often contain a variety of frequency information, which are typical multi-component signals. And the nonlinear coupling between aeroacoustics noise and environmental background noise results in nonlinear components in the acquisition signals. The empirical mode decomposition (EMD) proposed by Huang *et al.* [25], [26] is an effective method to deal with non-linear and non-stationary signals. The EMD method does not need to pre-set the basis functions, unlike Fourier transform [27], wavelet [28] and other analysis methods, the decomposition process is completely adaptive, and no longer subject to Heisenberg uncertainty principle, so it can better describe and extract the nonlinear and non-stationary features of the signals. However, the classical EMD method has problems of ''endpoint effect'' and poor noise robustness. Afterwards many improved algorithms, such as ensemble empirical mode decomposition (EEMD) [29], complementary ensemble empirical mode decomposition (CEEMD) [30], were proposed. EMD and its improved algorithms have advantages in analyzing nonlinear and non-stationary signals, so they are also widely used in blind source separation. B. Mijovic *et al.* proposed a single channel blind source separation (SCBSS) method combining EMD / EEMD with independent component analysis (ICA), and considered that the performance of the SCBSS was better than that of single channel ICA (SCICA) and wavelet ICA (WICA) at low signal-to-noise ratio (SNR) [31]. He and Chen [32] proposed a single channel blind source separation method based on EMD, and by calculating the decomposed intrinsic mode function (IMF) correlation matrix, the eigenvalue was used to determine the number of sources, then the source signals were separated by the non-negative matrix factorization (NMF). Aiming at problems of EMD and EEMD, D. Wang *et al.* proposed an enhanced EEMD method, which was applied to extract periodic and random instantaneous components of single channel vibration signals.

Although widely applied, EMD and its improved algorithms are empirical, and there is no complete mathematical theory basis [34], [35]. Dragomiretskiy and Zosso [36] proposed a variational mode decomposition (VMD) in 2014, and different from EMD and other improved methods, the VMD transforms the decomposition process into non-recursive, variational problems to solve, which has the theoretical support, at the same time, the VMD has better noise robustness. Dey *et al.* [37] introduced a method based on VMD and principal component analysis (PCA) for single channel blind source separation. However, after dimension reduction and compression by PCA [38], [39], the interpretability of the original sample data is reduced because non-principal components may also contain important information about signals features. Tang *et al.* [40] proposed a new underdetermined blind source separation method by using VMD and ICA, and the suggested method has high adaptability and practicability under strong noise interference, therefore, the method has been applied to mechanical fault diagnosis and analysis [41], [42]. However, the background noise of wind turbine aeroacoustics signals is much more complicated than that of mechanical vibration signals. If the number of modes extracted from VMD, i.e. the parameter K defined in [36], is not selected properly before ICA, it will have an extreme impact on the feature extraction of aeroacoustics signals and the noise robustness of the algorithm. The above researches do not provide effective solutions, so there are some limitations in wind turbine aeroacoustics signals processing by using the existing methods directly. Also, there is no widely accepted method for determining the optimal K of VMD. W. X. Wu *et al.* proposed a method of determining the optimal number of modes of VMD by means of maximizing kurtosis of the modes that have maximum correlations with the original signal [43]. Ren *et al.* [44] took energy differences between the original signal and the restructured signal after VMD as the evaluation parameter to determine the optimal number of modes. Mao *et al.* [45] proposed an improved parameter-adaptive VMD (IPAVMD) to solve the optimal number of modes issues and enhance algorithm performance by combining with kurtosis and the envelope spectrum kurtosis, which takes the stationarity and impulsiveness of signals into consideration simultaneously. Zhang *et al.* [46] used the maximum weighted kurtosis index constructed by kurtosis and correlation coefficient to optimize the VMD parameters. Indeed, these methods have some optimization effect under

their respective research background. However, there is no related report on how to determine the VMD parameter K for wind turbine aeroacoustics signals processing.

In this paper, a single channel blind source separation (SCBSS) method based on VMD is proposed and applied to the separation of wind turbine aeroacoustics signals which is collected by a single acoustic sensor. The VMD method decomposes nonlinear and non-stationary signals completely from the data itself, which is adaptive. And VMD improves the problems of mode mixing and "endpoint effect" of classical EMD, also it has a complete mathematical basis. And in order to improve the noise robustness of the algorithm, we propose a novel method to determine the number of modes of VMD combined correlation coefficients with the overall index of orthogonality. The problem of single channel underdetermined blind source separation is transformed into a non-underdetermined problem by constructing virtual multi-channel signals of the observed signals with VMD. And the joint approximate diagonalization of eigen-matrices of fourth-order cumulant matrices [47], [48] is used to realize blind source separation.

The rest of this paper is organized as follows: Section II introduces mixing and separation models and the single channel blind source separation problems. Section III introduces the variational mode decomposition and the algorithm flow. In Section IV, we propose single channel blind source separation based on VMD and the method to determine the number of decomposed layers. In section V, we analyze and discuss the separation performance of the proposed VMD-BSS method and the existing methods through simulation signals. In section VI, we choose two sequences of the actual aeroacoustics signals of onshore and offshore wind turbines and use the proposed VMD-BSS to separate acoustic components. Section VII concludes on our work of the paper and puts forward the following optimization and future research directions.

II. SINGLE CHANNEL BLIND SOURCE SEPARATION

For n-dimension statistically independent source signals $\boldsymbol{S}(t) = [s_1(t), s_2(t), \cdots, s_n(t)]^{\mathrm{T}}$, we acquire m-dimension observed signals $\boldsymbol{X}(t) = [x_1(t), x_2(t), \cdots, x_m(t)]^{\mathrm{T}}$ from m sensors, and the transmission channel interference noise are $\boldsymbol{N}(t) = [n_1(t), n_2(t), \cdots, n_m(t)]^{\mathrm{T}}$. Considering that each signal is linear mixed when it is received by one sensor, of which we ignore the transmission time, a linear instantaneous mixing model can be described as follows:

$$\boldsymbol{X}(t) = \boldsymbol{A}\boldsymbol{S}(t) + \boldsymbol{N}(t) \tag{1}$$

where the $\boldsymbol{A} \in \mathbb{R}^{m\times n}$ is the blind mixing matrix, and the linear instantaneous mixing model is shown in Figure 1.

In fact, in most cases, the interference noise can also be regarded as a kind of source signal. Therefore, Equation (1) can be transformed into a noise-free model:

$$\boldsymbol{X}(t) = \boldsymbol{A}\boldsymbol{S}(t) \tag{2}$$

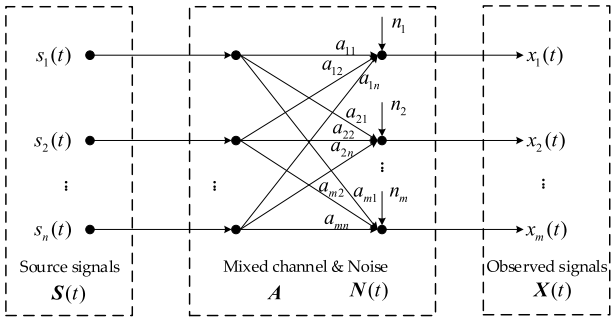

FIGURE 1. The linear instantaneous mixing model.

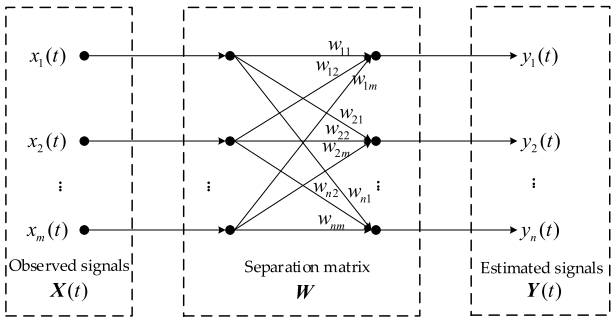

FIGURE 2. The forward separation model.

The forward separation model is shown in Figure 2. There exists a separation matrix $\boldsymbol{W} \in \mathbb{R}^{n\times m}$, and the relation between observed signals $\boldsymbol{X}(t) = [x_1(t), x_2(t), \cdots, x_m(t)]^{\mathrm{T}}$ and output signals (estimation of source signals) of separation system $\boldsymbol{Y}(t) = [y_1(t), y_2(t), \cdots, y_n(t)]^{\mathrm{T}}$ is:

$$\boldsymbol{Y}(t) = \boldsymbol{W}\boldsymbol{X}(t) \tag{3}$$

The purpose of blind source separation is to find or estimate the separation matrix $\boldsymbol{W}$. According to the numbers of observed signals and source signals, the blind source separation problems can be divided into overdetermined case ($m > n$), determined case ($m = n$) and underdetermined case ($m < n$). Only when the mixing matrix $\boldsymbol{A}$ is nonsingular, i.e. $m \geq n$, is it possible to find its inverse matrix or generalized inverse matrix $\boldsymbol{W}$ to realize the separation of signals. Therefore, it is a necessary condition for reverse of the mixing process that the number of observed signals is greater than or equal to the number of source signals. For the determined case, there are many reports and mature researches. For the overdetermined case, the number of observed signals can always be reduced to the same number as the source signals (determined cases), and then separated by methods of the determined case. However, for the underdetermined case, it is most consistent with the actual process, and the problem is more complex. The single channel problem is the extreme case of the underdetermined case [49].

III. VARIATIONAL MODE DECOMPOSITION

Similar to the definition of IMF in EMD, but the variational mode decomposition (VMD) [36] assumes that each mode

has a finite bandwidth with different central frequencies [50]. In order to minimize the sum of the estimated bandwidth of the modes, it transforms to solve functional variational problems. The alternate direction method of multipliers (ADMM) is used to update the modes and central frequencies in the frequency domain, and then the modes and the corresponding central frequencies are extracted. Compared with EMD, VMD has better performance in mode mixing reduction and noise robustness. At the same time, the VMD transforms the decomposition process into non-recursive, variational problems to solve, which has theoretical support.

In the VMD, the variational problem is described as: under the constraint that the sum of the modes is equal to the original signal $x(t)$, the sum of the estimated bandwidths of the modes is minimized. The process is as follows:

(i) Calculate the analytic signal [51] of each mode and its unilateral spectrum by means of the Hilbert transform:

$$\left(\delta(t)+\frac{j}{\pi t}\right)*x_k(t) \tag{4}$$

(ii) Estimate the center frequency ω_k of each mode and shift the mode's frequency spectrum to baseband:

$$\left[\left(\delta(t)+\frac{j}{\pi t}\right)*x_k(t)\right]e^{-j\omega_k t} \tag{5}$$

(iii) Calculate the squared L^2-norm of the gradient of the above demodulation signal, and estimate the bandwidth of each mode. The variational constraint problem is as follows:

$$\begin{aligned}&\min_{\{x_k\},\{\omega_k\}}\left\{\sum_k\left\|\partial_t\left[\left(\delta(t)+\frac{j}{\pi t}\right)*x_k(t)\right]e^{-j\omega_k t}\right\|_2^2\right\}\\&s.t.\ \sum_k x_k(t)=x(t)\end{aligned} \tag{6}$$

where $\{x_k\}=\{x_1,x_2,\cdots x_K\}$ and $\{\omega_k\}=\{\omega_1,\omega_2,\cdots\omega_K\}$ are shorthand notations for the set of all modes of VMD and corresponding center frequencies.

In order to solve the variational problem, the penalty term α and Lagrangian multipliers $\lambda(t)$ are introduced, and the constrained variational problem is converted to a non-constrained variational problem. The penalty term α ensures the accuracy of signal reconstruction under the Gaussian noise and the Lagrangian multipliers $\lambda(t)$ is used to enforce constraints strictly. The augmented Lagrangian L is the following [52]:

$$\begin{aligned}&L\left(\{x_k\},\{\omega_k\},\lambda\right)\\&=\alpha\sum_k\left\|\partial_t\left[\left(\delta(t)+\frac{j}{\pi t}\right)*x_k(t)\right]e^{-j\omega_k t}\right\|_2^2\\&\quad+\left\|x(t)-\sum_k x_k(t)\right\|_2^2+\left\langle\lambda(t),x(t)-\sum_k x_k(t)\right\rangle\end{aligned} \tag{7}$$

To find the saddle point of the augmented Lagrangian L, alternate direction method of multipliers (ADMM) [53] is used to update x_k^n, ω_k^n and λ^n, where n is the update count. The algorithm flow of VMD is shown in Figure 3.

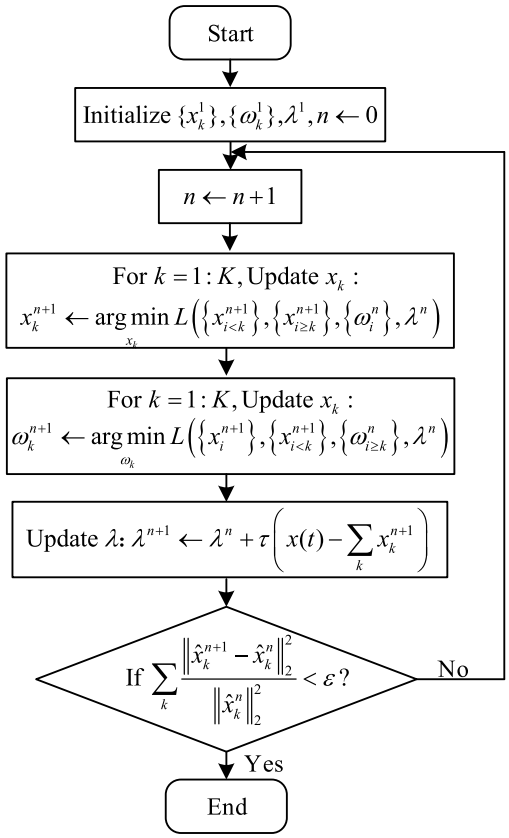

FIGURE 3. The algorithm flow of variational mode decomposition.

IV. PROPOSED METHOD

In the acquisition process of actual wind turbine aeroacoustics signals, the signals collected by a single acoustic sensor is a typical single channel mixing model. For the convenience of the research, we assume that the mixing process is in line with the linear instantaneous mixing model.

In the case of single channel underdetermined, the inverse matrix of the mixing matrix $\boldsymbol{A}$ does not exist and even if the mixed matrix is known, the separation of source signals is not unique. Therefore, the classical non-underdetermined blind source separation method cannot directly solve the single channel blind source separation problem. In this paper, we propose a novel virtual multi-channel method to increase the dimension of single channel observed signals by VMD, then use the non-underdetermined blind source separation method to find the optimal estimation of source signals.

A. IMPROVED VARIATIONAL MODE DECOMPOSITION

The number of decomposed layers should be determined in advance in VMD. Some research has shown that if the number of decomposed layers is small, the multi-scale features in original signal may be decomposed into the same mode, or even a mode cannot be decomposed. On the contrary, if the number of decomposed layers is too large, the same scale features will be decomposed into different modes, and the problem of over-decomposition will occur. However, at present, there is no effective method to determine the decomposition

layers of VMD. In this paper, we propose a new method, which combines correlation coefficients between decomposition components and observed signals and the overall index of orthogonality, to determine the number of decomposition layers of VMD.

1) CORRELATION CRITERION

For time sequences $x(t)$ and $y(t)$, of which statistical expectations are 0, with the same sampling frequencies and lengths, the correlation coefficients of them are defined as:

$$\rho_{xy} = \frac{\sum_{t=0}^{T} x(t)y(t)}{\sqrt{\sum_{t=0}^{T} x^2(t)}\sqrt{\sum_{t=0}^{T} y^2(t)}} \tag{8}$$

For given number of the decomposed layers K, the correlation coefficients of each mode $x_i(t)$ and the original observed signal $x(t)$ is:

$$\rho_{xx_i} = \frac{\sum_{t=0}^{T} x(t)x_i(t)}{\sqrt{\sum_{t=0}^{T} x^2(t)}\sqrt{\sum_{t=0}^{T} x_i^2(t)}} \tag{9}$$

When the correlation coefficients of some modes and the observed signal are obviously small, it can be judged that these modes are illusive components and the observed signal is over-decomposed, which need to reduce the number of decomposition layers K.

2) OVERALL INDEX OF ORTHOGONALITY CRITERION

The index orthogonality between any two IMFs in EMD method [25] is defined as follows:

$$IO_{i,j} = \sum_{t=0}^{T} \frac{x_i(t)x_j(t)}{x_i^2(t) + x_j^2(t)} \tag{10}$$

and the overall index of orthogonality is described as:

$$IO = \sum_{t=0}^{T}\left(\sum_{i=1}^{K}\sum_{j=1}^{K} x_i(t)x_j(t)/x^2(t)\right), \quad (i \neq j) \tag{11}$$

We introduce the IO criterion to judge the orthogonality of decomposition results of VMD. The orthogonality between different modes of VMD is worse, when the value of the IO is larger. And on the contrary, the smaller the value of the IO, the better the orthogonality of decomposition results it is, especially for $IO = 0$, all modes of VMD are completely orthogonal. When K is adjusted to minimum IO, the current K can be considered as the optimal number of decomposed layers.

B. VIRTUAL MULTI-CHANNEL SIGNALS

Combined with the VMD method and the above two decomposition criterions, the optimal number of the decomposition layers is determined and the observed signal is decomposed. And the virtual multi-channel signals of single channel observed signals are built as follows:

$$\boldsymbol{X}(t) = [x_1(t), x_2(t), \cdots, x_m(t)]^{\mathrm{T}} \tag{12}$$

The VMD method has the advantage of decomposing components with different time-frequency features. In other words, the VMD of observed signal is the process of decomposing different time-frequency features. Furthermore, the decomposed modes of the observed signals contain different features of the source signals. Different from VMD-PCA method, the improved VMD method combined with correlation criterion and overall index of orthogonality criterion not only has the abilities of component analysis, but more importantly has higher reconstruction accuracy than VMD-PCA method. Remarkably, the virtual multi-channel signals can completely reconstruct the observed signal, so hereinafter the virtual multi-channel signals and observed signal mean the same thing without ambiguity.

C. JOINT APPROXIMATE DIAGONALIZATION OF EIGEN-MATRICES

1) WHITENING AND DECORRELATION

In fact, all the virtual multi-channel signals have some correlations, and the whitening can remove the correlations between them, so that the mixing matrix is reduced to an orthogonal matrix. After whitening, the convergence of the algorithm and stability are better.

The autocorrelation matrix [54] of virtual multi-channel signals reconstructed of observed signal is:

$$\boldsymbol{R}_X = E\left[\boldsymbol{X}(t)\boldsymbol{X}^{\mathrm{T}}(t)\right] \tag{13}$$

Obviously, the matrix $\boldsymbol{R}_X$ is a positive definite matrix with eigenvalue decomposition as follows:

$$\boldsymbol{R}_X = \boldsymbol{V}_X\boldsymbol{\Lambda}_X\boldsymbol{V}_X^{\mathrm{T}} \tag{14}$$

where the matrix $\boldsymbol{\Lambda}_X = \mathrm{diag}[\lambda_1, \lambda_2, \cdots \lambda_m]$ is a diagonal matrix consisting of eigenvalues of matrix $\boldsymbol{R}_X$ in descending order, and the matrix $\boldsymbol{V}_X$ is a orthogonal matrix composed of corresponding eigenvectors. Then we can get whitening matrix:

$$\boldsymbol{W}_0 = \boldsymbol{\Lambda}_X^{-\frac{1}{2}}\boldsymbol{V}_X^{\mathrm{T}} \tag{15}$$

If $\boldsymbol{Z}(t)$ is the observed signal after whitening, then there is:

$$\boldsymbol{Z}(t) = \boldsymbol{W}_0\boldsymbol{X}(t) \tag{16}$$

2) JOINT APPROXIMATE DIAGONALIZATION OF EIGEN-MATRICES

Four order cumulants [55] of the whitening signals $\boldsymbol{Z}(t)$ is defined as:

$$\begin{aligned} cum(z_i, z_j, z_k, z_l) = {} & E(z_iz_jz_kz_l) - E(z_iz_j)E(z_kz_l) \\ & - E(z_iz_k)E(z_jz_l) - E(z_iz_l)E(z_jz_k), \\ & (1 \leq i, j, k, l \leq m) \end{aligned} \tag{17}$$

And the four order cumulant matrix of whitening signal is:

$$\boldsymbol{C}_Z(\boldsymbol{M}) = \sum_{k,l=1}^{m} cum(z_i, z_j, z_k, z_l) m_{kl} \quad i,j = 1 \sim m \tag{18}$$

where the $m_{i,j}$ is the i,j element in the matrix $\boldsymbol{C}_Z(\boldsymbol{M})$. It can be proved that the four order cumulant matrix $\boldsymbol{C}_Z(\boldsymbol{M})$ can always be decomposed as $\boldsymbol{C}_Z(\boldsymbol{M}) = \nu\boldsymbol{M}$, where the ν and $\boldsymbol{M}$ are eigenvalue and eigenmatrix of $\boldsymbol{C}_Z(\boldsymbol{M})$ respectively.

From the definition of the four order cumulant matrix, we know that $\boldsymbol{C}_Z(\boldsymbol{M})$ is a symmetric matrix. Therefore, there must be an orthogonal normalized matrix $\boldsymbol{U}$, which makes the four order cumulant matrix $\boldsymbol{C}_Z(\boldsymbol{M})$ diagonalized:

$$\boldsymbol{U}\boldsymbol{C}_Z(\boldsymbol{M})\boldsymbol{U}^{\mathrm{T}} = \mathrm{diag}[\nu_1, \nu_2, \cdots \nu_m] \tag{19}$$

In practical, in order to suppress noise and calculation error, we select pm^2-dimension matrix $\boldsymbol{M}_i$ $(1 \le i \le p \le m)$, and calculate each fourth order cumulant matrix $\boldsymbol{C}_Z(\boldsymbol{M}_i)$. Then we calculate the $\boldsymbol{U}$ which can diagonalize any $\boldsymbol{C}_Z(\boldsymbol{M}_i)$. It is difficult to achieve complete diagonalization, so we choose the sum of squares of $\boldsymbol{U}\boldsymbol{C}_Z(\boldsymbol{M}_i)\boldsymbol{U}^{\mathrm{T}}$ diagonal elements, i.e.

$$C(\boldsymbol{U}) = \sum_{i=1}^{P} \left|\mathrm{diag}[\boldsymbol{U}^{\mathrm{T}}\boldsymbol{C}_Z(\boldsymbol{M}_i)\boldsymbol{U}]\right|^2 \tag{20}$$

as the criterion [56],[57] to achieve approximate diagonalization. Then we get the eigenmatrix $\boldsymbol{U}$ by means of minimizing $C(\boldsymbol{U})$ using the Jacobian rotation [58]. And the estimation of source signals is as follows:

$$\boldsymbol{Y}(t) = \boldsymbol{U}^{\mathrm{T}}\boldsymbol{W}_0\boldsymbol{X}(t) \tag{21}$$

D. EVALUATION CRITERION OF SEPARATION RESULTS

In order to evaluate the separation effect, the correlation coefficients between the source signals $\boldsymbol{S}(t)$ and separated signals $\boldsymbol{Y}(t)$, i.e. estimation of source signals, are used as the separation criterion, which are defined as:

$$\rho_{s_i y_i} = \frac{\sum_{t=0}^{T} s_i(t) y_i(t)}{\sqrt{\sum_{t=0}^{T} s_i^2(t)} \sqrt{\sum_{t=0}^{T} y_i^2(t)}} \tag{22}$$

The correlation coefficients are unaffected about amplitude differences between source signals and estimated signals after blind source separation. And the $\left|\rho_{s_i y_i}\right|$ closer to 1, the effect of blind source separation is the better.

V. SIMULATION SIGNALS ANALYSIS AND DISCUSSION

In this section, the effectiveness of the proposed method is verified by simulation signals example. The simulation signals $\boldsymbol{S}(t)$ consist of three source signals and a Gauss transmission noise, i.e. $\boldsymbol{S}(t) = [s_1(t), s_2(t), s_3(t), \eta]^{\mathrm{T}}$, and more specifically:

$$\begin{cases} s_1(t) = \cos(2\pi f_0 t + \pi f_0 t^2) \\ s_2(t) = \cos(20\pi f_0 t + 0.2\cos(\pi f_0 t)) \\ s_3(t) = \cos(10\pi f_0 t) \\ \eta \sim N(0, \sigma^2) \end{cases} \tag{23}$$

where $f_0 = 10Hz$, and Gauss noise intensity can be determined by controlling the standard deviation σ. Suppose the signal sampling frequency of a single sensor is 1024 Hz, and the signal length is 1024 sampling points. The source signals $s_1(t)$ and $s_2(t)$ are non-stationary signals, and $s_3(t)$ is a stationary signal. The noise parameter σ is 0.01. The time-frequency waveform of $\boldsymbol{S}(t)$ is shown in Figure 4.

For designated mixing matrix $\boldsymbol{A} = [0.53, 0.23, 0.69, 1]$, a single channel observed signal $x(t)$ maxed by sources and noise signals is obtained by means of Equation (2). And its time-frequency distribution is shown in Figure 5.

A. VIRTUAL MULTI-CHANNEL SIGNALS

The difference of the number of decomposed layers will directly affect the decomposition result of single channel observed signals, and then affect the results of blind source separation. The correlation criterion and overall index of orthogonality criterion, which we have discussed in Section IV, are used to determine the number of decomposition layers.

The correlation coefficients $|\rho|$ between the observed signal and each mode under different number of decomposition layers are shown in Table 1. Evidently, the correlation coefficients between each mode and the observed signal vary with the number of decomposed layers. When $K = 2, 3, 4$, there are strong correlations between each mode and observed signal. When $K = 4$, that further analysis of the correlation coefficient between the 2nd and 3rd modes shows they are almost the same mode, of which correlation coefficient has reached to 0.9983, so it can be judged that it is over-decomposed. Similarly, when $K = 5$, the correlation coefficient between the 3rd and 4th modes is 0.9909, which is over-decomposed, and the correlation coefficient between the 5th mode and the observed signal is not remarkable enough, so it can be judged as a "false mode". Therefore, the number of decomposed layers, i.e. $K = 3$, can be roughly judged through the correlation criterion.

TABLE 1. Correlation coefficients of each mode and the observed signal under different decomposed levels.

K	ρ_1	ρ_2	ρ_3	ρ_4	ρ_5
2	0.5955	0.7821			
3	0.5902	0.7866	0.2563		
4	0.5896	0.7751	0.7705	0.2566	
5	0.5899	0.7696	0.2593	0.2577	0.0144

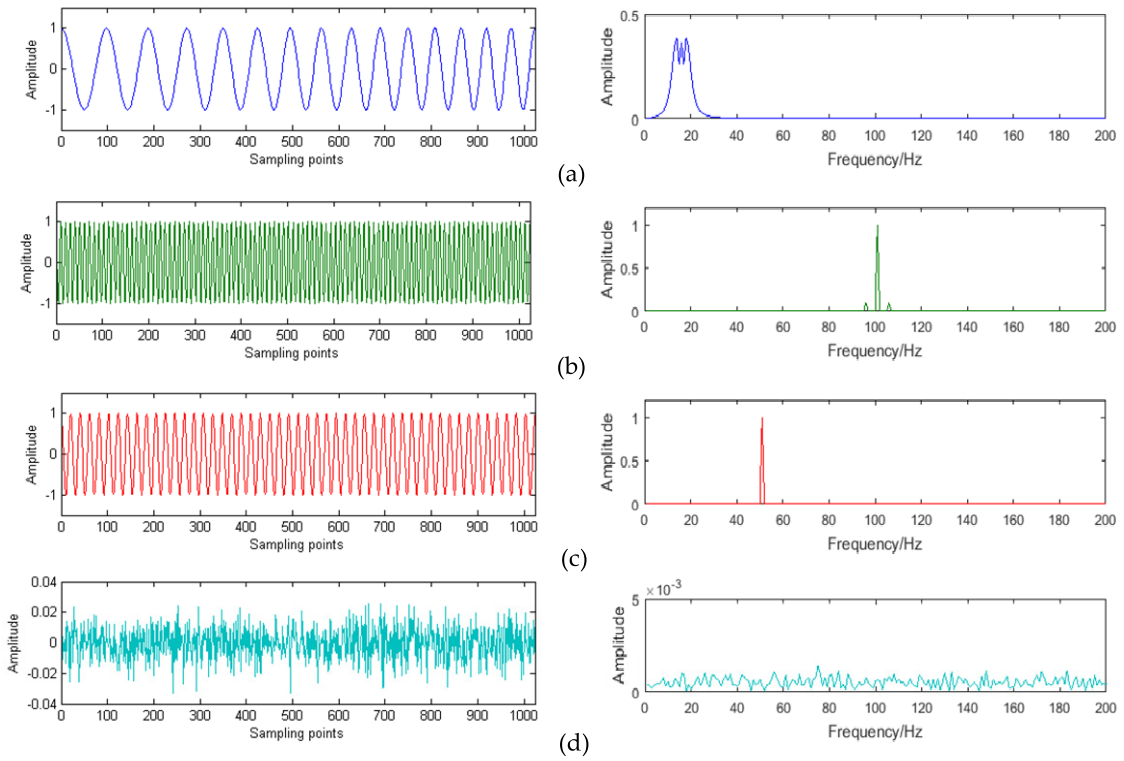

FIGURE 4. The time-frequency waveform of $S(t)$: (a) The time-frequency waveform of $s_1(t)$; (b) The time-frequency waveform of $s_2(t)$; (c) The time-frequency waveform of $s_3(t)$; (d) The time-frequency waveform of Gauss noise $\eta \sim (0, \sigma^2)$.

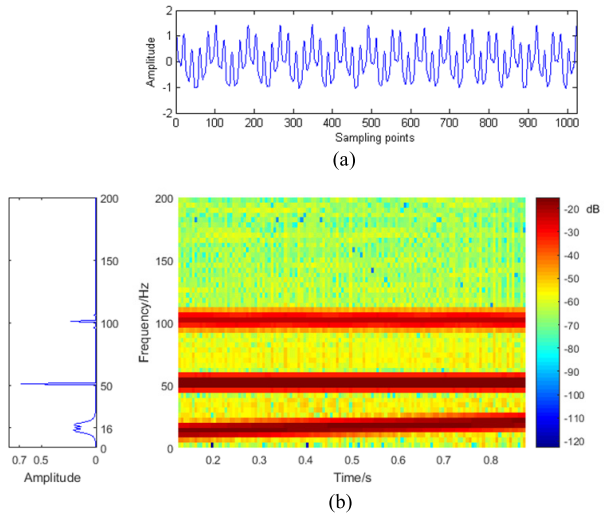

FIGURE 5. The time-frequency distribution of $x(t)$: (a) The waveform of $x(t)$ in time domain; (b) The time-frequency distribution of $x(t)$.

The overall index of orthogonality criterion is used to test the orthogonality of the modes decomposed under different number of decomposition layers, and the IO values under different K is shown in Table 2. The IO of different number of decomposition layers are very close to 0, so the modes decomposed by VMD are approximately orthogonal. When $K = 3$, the IO is the smallest, and the orthogonality is the best.

TABLE 2. Overall index of orthogonality under different number of decomposed layers.

K	2	3	4	5
IO	1.606×10^{-3}	2.046×10^{-5}	4.360×10^{-4}	8.360×10^{-4}

If the number of decomposition layers increases or decreases, the IO value will increase and the decomposition orthogonality will be worse. Considering the correlation criterion and overall index of orthogonality criterion comprehensively, we can get the optimal number of decomposition layers, that is $K = 3$.

The VMD decomposition results of the observed signal are shown in Figure 6 (a), and Figure 6 (b) is the decomposition results of the EMD method to compare the decomposition performance of the VMD and EMD methods. Because the orders of modes or IMFs decomposed by VMD or EMD are different, which have no effect on the reconstruction of the signal, so we adjust their orders to be consistent with the corresponding components of observed signal for convenience. Compared with EMD, the VMD is more effective in separating non-stationary signals ($x_1(t)$ and $x_2(t)$), and the separated components are better "fit" with the corresponding components of the observed signals. For stationary signal ($x_3(t)$), both of VMD and EMD have good performance, and can recognize the corresponding component of the observed

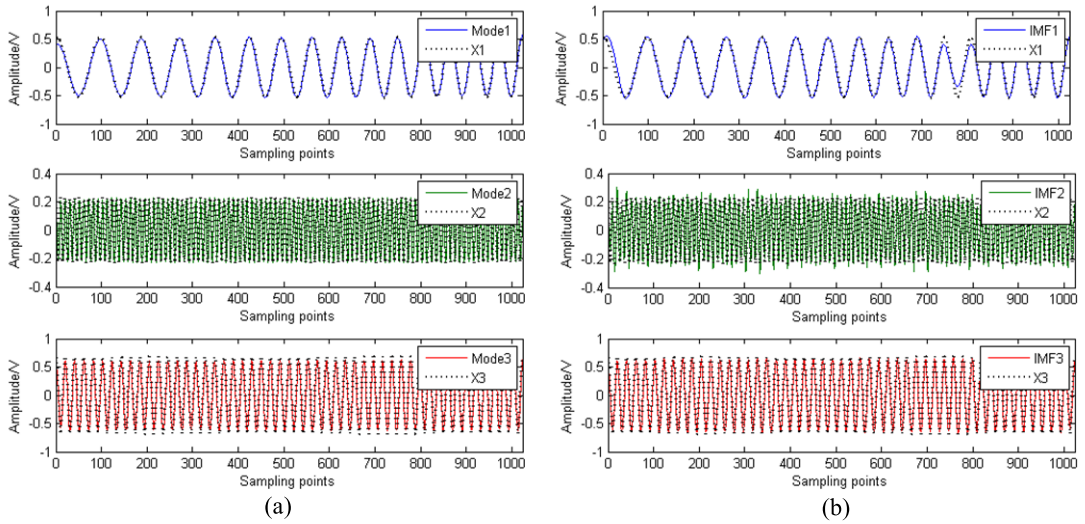

FIGURE 6. Decomposition results of VMD and EMD: (a) Modes of VMD; (b) IMFs of EMD.

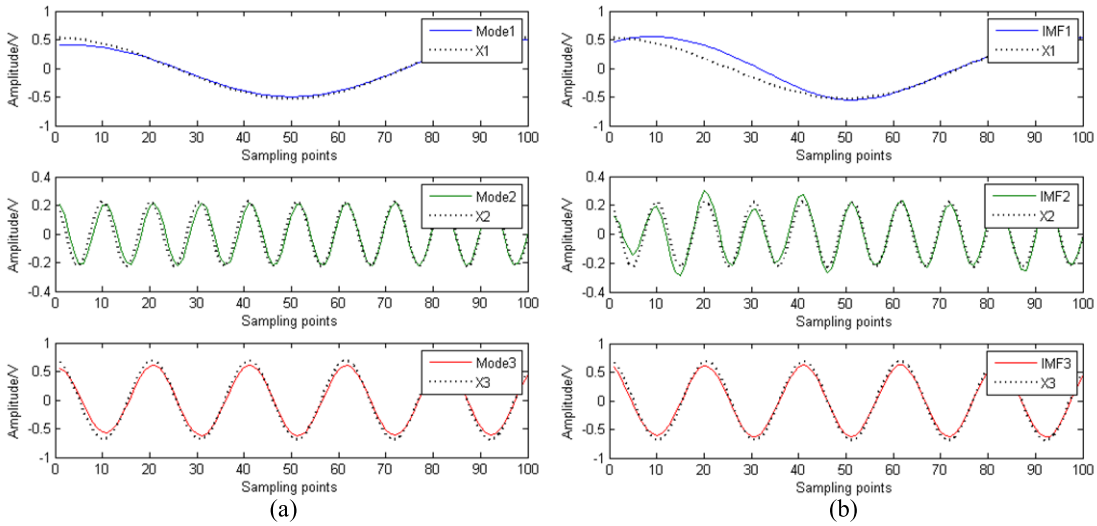

FIGURE 7. Decomposition near the endpoints of VMD and EMD: (a) Modes of VMD; (b) IMFs of EMD.

signal very well. The separation effect of VMD and EMD at the endpoint is shown in Figure 7. In terms of ''endpoint effect'', the advantage of the VMD method is obvious. The ''endpoint effect'' of the three modes decomposed by the VMD are all controlled within 15 sampling points, while for EMD, the ''endpoint effect'' of two non-stationary signals (IMF1 and IMF2) have reached 100 sampling points and 46 sampling points respectively.

B. SINGLE CHANNEL BLIND SOURCE SEPARATION BASED ON VMD

After VMD of the observed signal, we obtain the virtual multi-channel signals, and then the blind source separation is realized by joint approximate diagonalization of eigenmatrices (JADE). The waveforms in time domain of the separated signals $\boldsymbol{Y}(t)$ are shown in Figure 8(a). In order to show the advantages of the proposed method, the separation effects of EMD-BSS and EEMD-BSS based on PCA are compared, as shown in Figure 8(b) and Figure 8(c), respectively. Because the order difference of the separated signals does not affect the separation results, the order of the separated signals is arranged according to the order of the source signals for convenience.

All the three methods can achieve blind source separation for simulation signals. The amplitudes of the separated signals are uncertain after blind source separation. And the correlation coefficients between the separated signals and the source signals can be used to judge the performance of each method quantitatively. The correlation coefficients between the separated signals and the source signals are shown in Table 3. It can be seen that the average correlation coefficient of the VMD-BSS method between separated signals

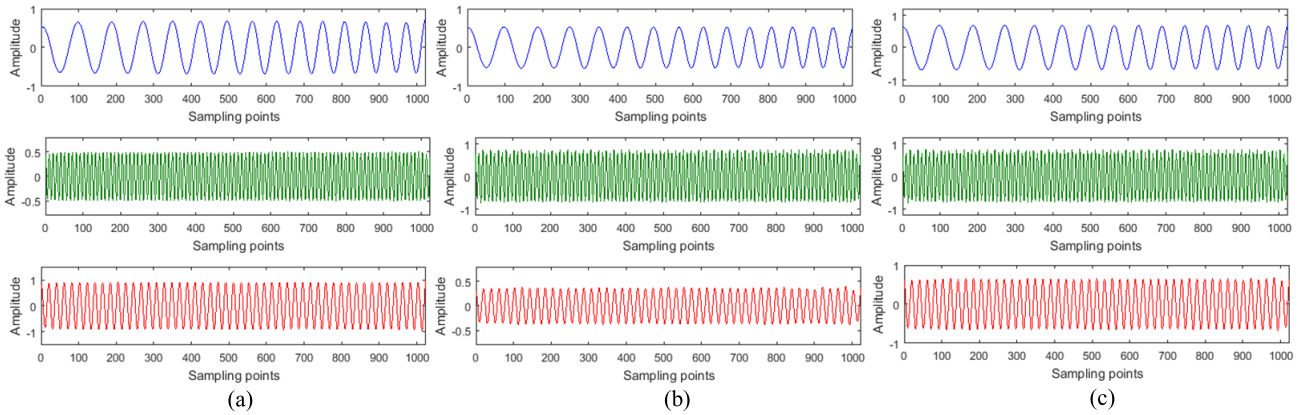

FIGURE 8. Separation effects of three BSS methods: (a) Separation effects of VMD-BSS; (b) Separation effects of EMD-BSS; (c) Separation effects of EEMD-BSS.

TABLE 3. Correlation coefficients of separated signals and source signals based on three BSS methods.

	$y_1(t)\,\|\,s_1(t)$	$y_2(t)\,\|\,s_2(t)$	$y_3(t)\,\|\,s_3(t)$	$y_4(t)\,\|\,s_4(t)$
Proposed Method	0.9136	0.9102	0.9433	0.9223
EMD-BSS	0.8969	0.8532	0.9316	0.8939
EEMD-BSS	0.9112	0.8975	0.9436	0.9174

TABLE 4. Time-cost of three BSS methods.

	Proposed Method	EMD-BSS	EEMD-BSS
Time-cost/s	0.201	0.143	9.850

FIGURE 9. Signals acquisition environments: (a) The onshore wind turbine; (b) The offshore wind turbine.

and the source signals is closer to 1, indicating that the separation performance is the most effective, while the average correlation coefficient of the EMD-BSS is not remarkable, and compared with the EMD-BSS method, the separation performance of the EEMD-BSS has improved. However, the EEMD-BSS requires multiple decompositions after additions of white noise, so it is much more time-consuming than VMD-BSS and EMD-BSS, especially when the amount of

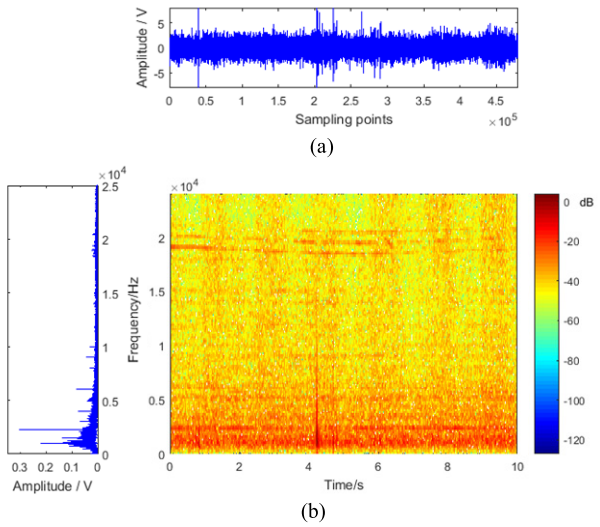

FIGURE 10. Actual aeroacoustics signals of the 1.5 MW wind turbine: (a) The waveform in time-domain of the actual signal; (b) The time-frequency distribution of the actual signal.

data is large. Table 4 lists the time-cost of the three methods on the MATLAB R2016a platform in the same case and the average number of EEMD is 100. The computer memory is 4GB and the CPU is Intel Core i3-2120 / 3.3GHz.

VI. ANALYSIS OF ACTUAL SIGNALS

The actual signals of wind turbine aeroacoustics signals in wind farms often mixed up other kinds of signals. In order to get pure aeroacoustics signals, the proposed VMD-BSS is a feasible method. In this section, we take the aeroacoustics signals of an onshore 1.5 MW wind turbine in Tsingtao, China and a 2.0 MW wind turbine in the intertidal zone of the East China Sea as research objects to discuss the proposed method of acoustics source blind separation and signals acquisition environments are shown in Figure 9. Limited by the acquisition conditions of the actual signals, the acoustic sensor is a single channel microphone with 16-bit ADC and 48 kHz sampling frequency. We choose 4.8×10^5 sampling

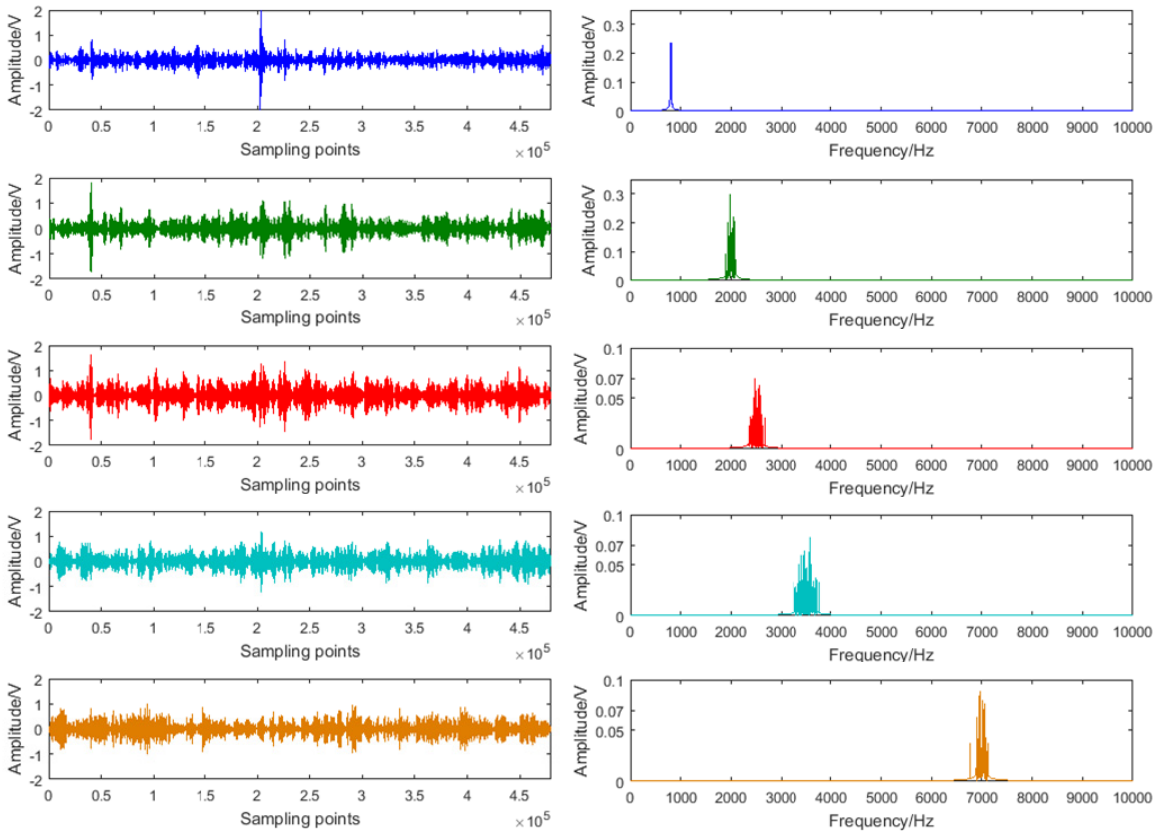

FIGURE 11. Results of the blind source separation of the 1.5 MW wind turbine.

points, i.e. 10s acoustic signals to analyze in each case. The acquired signals of acoustic sensor are not linear with the actual acoustic pressure, but has a monotone function relationship. That is, the waveform of acoustic pressure is similar to the waveform of the output voltage of the acoustic sensor, of which the frequencies are the same but the amplitudes are different. In fact, for aeroacoustics signals, the analysis of time-frequency characteristics is more useful. Therefore, we can analyze the output voltage directly.

A. CASE I: ACTUAL AEROACOUSTICS SIGNALS OF A 1.5 MW WIND TURBINE IN AN ONSHORE WIND FARM IN TSINGTAO, CHINA

1) ACQUISITION OF THE ACTUAL ACOUSTIC SIGNALS

Acquisition environment: Temperature, 16 °C; Relative humidity, 63%; Wind velocity, 8 ∼ 10 m/s; Hilly region.

The waveform in time-domain of the actual signal is shown in Figure 10(a), and the corresponding amplitude time-frequency characteristics are shown in Figure 10(b). In the frequency domain, the main frequency band of the acoustic signal is from 500 Hz to 5 kHz, and there are several central frequencies in this range. In time domain, the actual acoustic signal is extremely non-stationary in the whole sampling time interval, especially near 0.4s and 2s ∼ 3s due to the influence of wind noise.

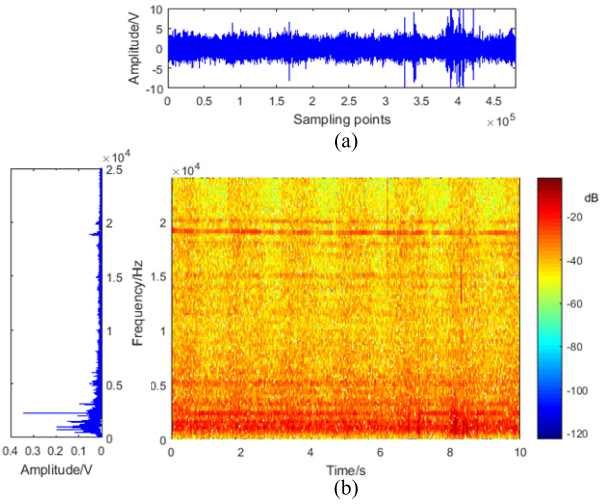

FIGURE 12. Actual aeroacoustics signals of the 2.0 MW wind turbine: (a) The waveform in time-domain of the actual signal; (b) The time-frequency distribution of the actual signal.

2) SEPARATION OF AEROACOUSTICS SOURCE SIGNALS BASED ON PROPOSED METHOD

The proposed method is applied to the blind separation of actual aeroacoustics signals, and 5 acoustic source signals

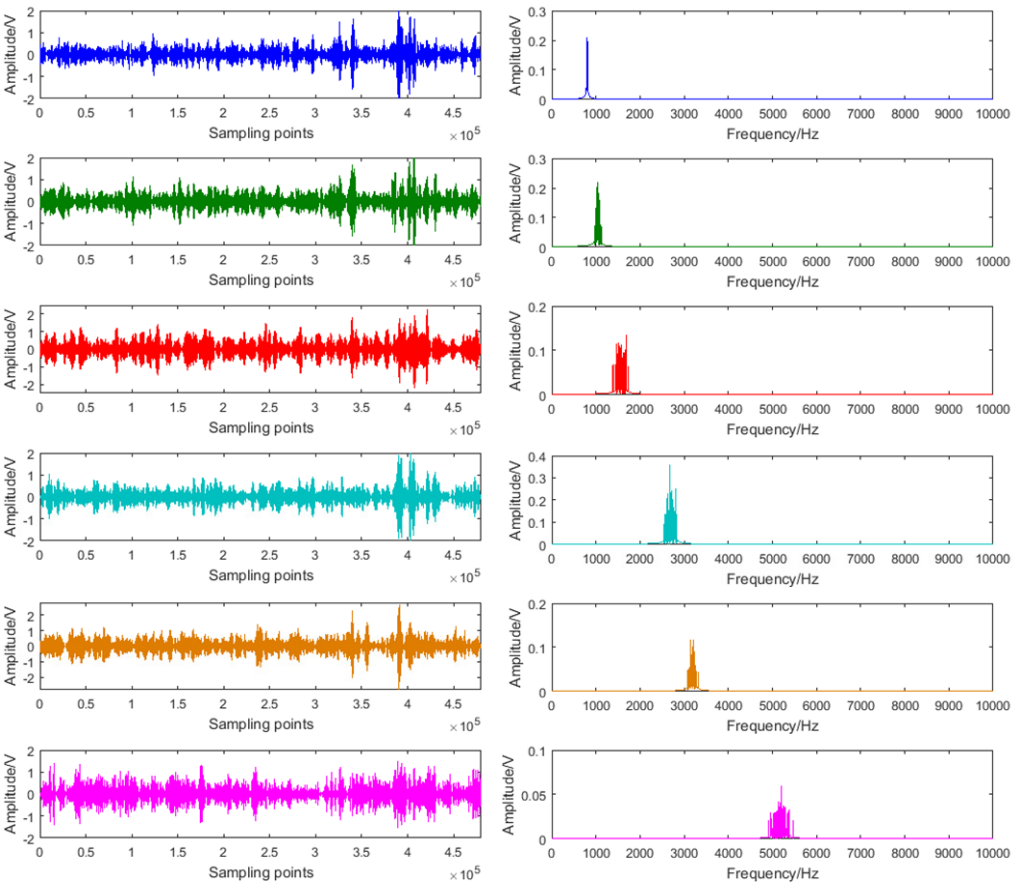

FIGURE 13. Results of the blind source separation of the 1.5 MW wind turbine.

are finally separated, as shown in Figure 11. The central frequencies are 812 Hz, 1983 Hz, 2437 Hz, 3506 Hz and 7009 Hz respectively, which are basically consistent with the time-frequency distribution characteristic in Figure 10. The original actual signal has strong noise interference. However, from the separation results, the proposed VMD-BSS in this paper can extract and separate the center frequencies of different acoustic sources accurately, and has strong noise robustness.

B. CASE II: ACTUAL AEROACOUSTICS SIGNALS OF A 2.0 MW WIND TURBINE IN THE INTERTIDAL ZONE OF THE EAST CHINA SEA

1) ACQUISITION OF THE ACTUAL ACOUSTIC SIGNALS

Acquisition environment: Temperature, 22 °C; Relative humidity, 92%; Wind velocity, 11 ∼ 15 m/s; Intertidal zone.

Similar to the analysis of Case I, the waveform in time-domain and the corresponding amplitude time-frequency characteristics of the 2.0 MW wind turbine actual aeroacoustics signals are shown in Figure 12(a) and 12(b) respectively. Unlike onshore environment, the acquired aeroacoustics signals signal of wind turbine in intertidal wind farm is also disturbed by marine environment noise and mechanical noise of working ships. In the frequency domain, the main frequency range of signals is concentrated between 500Hz ∼ 4kHz. In the time domain, there is a strong influence of wind noise near 7.2s, followed by a strong interference of sea wave noise near 8s.

2) SEPARATION OF AEROACOUSTICS SOURCE SIGNALS BASED ON PROPOSED METHOD

The actual aeroacoustics signals of the 2.0 MW wind turbine in intertidal wind farm are finally separated into 6 sources by the proposed VMD-BSS, as shown in Figure 13. The central frequencies are 726Hz, 1034Hz, 1569Hz, 2697Hz, 3165Hz and 5192Hz respectively. The center frequency 726Hz and 1034Hz is close, but it can be seen from the separation results that there is almost no frequency mixing.

VII. CONCLUSIONS

The acquisition and measurement of aeroacoustics signals of wind turbine are important for environmental noise assessment and blades fault detection. However, the operating environment of wind turbines determines that lots interference noise signals would be mixed up. Therefore, it is necessary to find out corresponding signal processing methods for

pure aeroacoustics signals signal separation. In this paper, we proposed a novel blind source separation method based on VMD for single channel wind turbine aeroacoustics signals separation. The correlation criterion and overall index of orthogonality criterion are used to determine the optimal number of decomposition layers of VMD. Then the virtual multi-channel signals of the observed signal are built. And finally, the separation is realized by means of the joint approximate diagonalization of eigen-matrices of fourth order cumulant matrices.

The VMD method has advantages in dealing with non-stationary and non-linear multi-component signals, and also has obvious performance in suppressing mode mixing and endpoint effect. The number of decomposition layers is one of the important parameters of VMD method, which directly affects the decomposition effect and the result of blind source separation. The method proposed in this paper, which combines the correlation criterion with the overall index of orthogonality criterion, can determine the number of decomposition layers more appropriately. The simulation results show that the VMD method is superior to the classical EMD method in suppressing the endpoint effect. Compared with separation performance of VMD-BSS, EMD-BSS and EEMD-BSS, the average recognition accuracy of VMD-BSS is 92.23%, which is higher than EMD-BSS and EEMD-BSS, and the computation time of VMD-BSS is much lower than EEMD-BSS. The suggested method is used for analysis of aeroacoustics signals of an onshore 1.5 MW wind turbine in Tsingtao, China and a 2.0 MW wind turbine in the intertidal zone of the East China Sea. It can accurately separate the acoustic source signals in accordance with frequency characteristics under strong noise interference and has excellent noise robustness. There is no obvious overlap in the frequency range of the separated source signals, indicating that the VMD method has a significant effect on suppressing mode mixing. At the same time, the non-stationary features of the source signals are preserved in separated components sufficiently, and the proposed method is adaptive.

It should be noted that the computational complexity of this method is considerable in the case of large amount of data. In fact, when dealing with actual signals, we segmented them to satisfy the limitation of computer performance. Nevertheless, the computer was still very laborious. In the real-time analysis of signals, the applicability still needs to be improved. Therefore, efficient simplification algorithms will be our important research direction in the future.

REFERENCES

[1] P. Y. Chen and T. Thiringer, "Analysis of energy curtailment and capacity overinstallation to maximize wind turbine profit considering electricity price–wind correlation," *IEEE Trans. Sustain. Energy*, vol. 8, no. 4, pp. 1406–1414, Oct. 2017.

[2] S. Sulaeman, M. Benidris, J. Mitra, and C. Singh, "A wind farm reliability model considering both wind variability and turbine forced outages," *IEEE Trans. Sustain. Energy*, vol. 8, no. 2, pp. 629–637, Apr. 2017.

[3] V. Katinasn, M. Marčiukaitis, and M. Tamašauskienė, "Analysis of the wind turbine noise emissions and impact on the environment," *Renew. Sustain. Energy Rev.*, vol. 58, pp. 825–831, May 2016.

[4] M. S. Campobasso, E. Minisci, and M. Caboni, "Aerodynamic design optimization of wind turbine rotors under geometric uncertainty," *Wind Energy*, vol. 19, no. 1, pp. 51–65, Jan. 2016.

[5] G. R. Pirrung, H. A. Madsen, T. Kim, and J. Heinz, "A coupled near and far wake model for wind turbine aerodynamics," *Wind Energy*, vol. 19, no. 11, pp. 2053–2069, Nov. 2016.

[6] S. Lee, "Numerical modeling of wind turbine aerodynamic noise in the time domain," *J. Acoust. Soc. Amer.*, vol. 133, no. 2, pp. 94–100, Feb. 2013.

[7] N. Sedaghatizadeh, M. Arjomandi, B. Cazzolato, and R. Kelso, "Wind farm noises: Mechanisms and evidence for their dependency on wind direction," *Renew. Energy*, vol. 109, pp. 311–322, Aug. 2017.

[8] W. Y. Liu, "A review on wind turbine noise mechanism and de-noising techniques," *Renew. Energy*, vol. 108, pp. 311–320, Aug. 2017.

[9] S. Gantasala, J. C. Luneno, and J. O. Aidanpää, "Influence of icing on the mode behavior of wind turbine blades," *Energies*, vol. 9, no. 11, p. 862, Nov. 2016.

[10] S. Buck, S. Oerlemans, and S. Palo, "Experimental characterization of turbulent inflow noise on a full-scale wind turbine," *J. Sound Vib.*, vol. 385, pp. 219–238, Dec. 2016.

[11] R. C. Ramachandran, G. Raman, and R. P. Dougherty, "Wind turbine noise measurement using a compact microphone array with advanced deconvolution algorithms," *J. Sound Vib.*, vol. 333, pp. 3058–3080, Jul. 2014.

[12] F. Bertagnolio, H. A. Madsen, and A. Fischer, "A combined aeroelastic-aeroacoustic model for wind turbine noise: Verification and analysis of field measurements," *Wind Energy*, vol. 20, no. 8, pp. 1331–1348, Aug. 2017.

[13] X. Huang, L. Yang, R. Song, and W. Lu, "Effective pattern recognition and find-density-peaks clustering based blind identification for underdetermined speech mixing systems," *Multimedia Tools Appl.*, vol. 77, no. 17, pp. 22115–22129, Sep. 2018.

[14] D. Kitamura *et al.*, "Generalized independent low-rank matrix analysis using heavy-tailed distributions for blind source separation," *EURASIP J. Adv. Signal Process.*, vol. 2018, p. 28, Dec. 2018.

[15] A. Nagathil, C. Weihs, K. Neumann, and R. Martin, "Spectral complexity reduction of music signals based on frequency-domain reduced-rank approximations: An evaluation with cochlear implant listeners," *J. Acoust. Soc. Amer.*, vol. 142, no. 3, pp. 1219–1228, Sep. 2017.

[16] R. B. Randall, "A history of cepstrum analysis and its application to mechanical problems," *Mech. Syst. Signal Process.*, vol. 97, pp. 3–19, Dec. 2017.

[17] Y. Hao, L. Song, Y. Ke, H. Wang, and P. Chen, "Diagnosis of compound fault using sparsity promoted-based sparse component analysis," *Sensors*, vol. 17, no. 6, pp. 1307-1–1307-16, Jun. 2017.

[18] G. D. Elia, M. Cocconcelli, E. Mucchi, and G. Dalpiaz, "Combining blind separation and cyclostationary techniques for monitoring distributed wear in gearbox rolling bearings," *Proc. Inst. Mech. Eng. C, J. Mech. Eng. Sci.*, vol. 231, no. 6, pp. 1113–1128, Mar. 2017.

[19] M. A. Haile and B. Dykas, "Blind source separation for vibration-based diagnostics of rotorcraft bearings," *J. Vib. Control*, vol. 22, no. 18, pp. 3807–3820, Oct. 2016.

[20] G. Gelle, M. Colas, and G. Delaunay, "Blind sources separation applied to rotating machines monitoring by acoustical and vibrations analysis," *Mech. Syst. Signal Process.*, vol. 14, no. 3, pp. 427–442, 2000.

[21] G. Gelle, M. Colas, and C. Serviere, "Blind source separation: A tool for rotating machine monitoring by vibrations analysis?" *J. Sound Vib.*, vol. 245, no. 5, pp. 865–885, Dec. 2001.

[22] M. J. Roan, J. G. Erling, and L. H. Sibul, "A new, non-linear, adaptive, blind source separation approach to gear tooth failure detection and analysis," *Mech. Syst. Signal Process.*, vol. 16, no. 5, pp. 719–740, Sep. 2002.

[23] S. I. McNeill and D. C. Zimmerman, "A framework for blind mode identification using joint approximate diagonalization," *Mech. Syst. Signal Process.*, vol. 22, no. 7, pp. 1526–1548, Oct. 2008.

[24] Y. C. Yang and S. Nagarajaiah, "Output-only mode identification with limited sensors using sparse component analysis," *J. Sound Vib.*, vol. 332, no. 19, pp. 4741–4765, Sep. 2013.

[25] N. E. Huang *et al.*, "The empirical mode decomposition and the Hilbert spectrum for nonlinear and non-stationary time series analysis," *Proc. Roy. Soc. London Ser. A, Math., Phys. Eng. Sci.*, vol. 454, no. 1971, pp. 903–995, Mar. 1998.

[26] N. E. Huang, Z. Shen, and S. R. Long, "A new view of nonlinear water waves: The Hilbert spectrum," *Annu. Rev. Fluid Mech.*, vol. 16, no. 5, pp. 719–740, Jan. 1999.
[27] D. Gabor, "Theory of communication," *J. Inst. Electr. Eng. I, Gen.*, vol. 94, p. 58, Jan. 1947.
[28] T. Christopher and G. P. Compo, "A practical guide to wavelet analysis," *Bull. Amer. Meteorol. Soc.*, vol. 79, no. 1, pp. 61–78, 1998.
[29] T. Wang, M. C. Zhang, Q. H. Yu, and H. Y. Zhang, "Comparing the applications of EMD and EEMD on time–frequency analysis of seismic signal," *J. Appl. Geophys.*, vol. 83, pp. 29–34, Aug. 2012.
[30] X. Xue, J. Zhou, Y. Zhang, W. Zhang, and W. Zhu, "An improved ensemble empirical mode decomposition method and its application to pressure pulsation analysis of hydroelectric generator unit," *Proc. Inst. Mech. Eng., O, J. Risk Rel.*, vol. 228, no. 6, pp. 543–557, Dec. 2014.
[31] B. Mijović, M. De Vos, I. Gligorijević, J. Taelman, and S. Van Huffel, "Source separation from single-channel recordings by combining empirical-mode decomposition and independent component analysis," *IEEE Trans. Biomed. Eng.*, vol. 57, no. 9, pp. 2188–2196, Sep. 2010.
[32] P. He and X. Chen, "A method for extracting fetal ECG based on EMD-NMF single channel blind source separation algorithm," *Technol. Health Care*, vol. 24, no. s1, pp. S17–S26, 2016.
[33] D. Wang, W. Guo, and P. W. Tse, "An enhanced empirical mode decomposition method for blind component separation of a single-channel vibration signal mixture," *J. Vib. Control*, vol. 22, no. 11, pp. 2603–2618, Jun. 2016.
[34] I. Daubechies, J. Lu, and H. T. Wu, "Synchrosqueezed wavelet transforms: An empirical mode decomposition-like tool," *Appl. Comput. Harmon. Anal.*, vol. 30, no. 2, pp. 243–261, Mar. 2011.
[35] J. Gilles, "Empirical wavelet transform," *IEEE Trans. Signal Process.*, vol. 61, no. 16, pp. 3999–4010, Aug. 2013.
[36] K. Dragomiretskiy and D. Zosso, "Variational mode decomposition," *IEEE Trans. Signal Process.*, vol. 62, no. 3, pp. 531–544, Feb. 2014.
[37] P. Dey, U. Satija, and B. Ramkumar, "Single channel blind source separation based on variational mode decomposition and PCA," in *Proc. Annu. IEEE India Conf. (INDICON)*, New Delhi, India, Dec. 2015, pp. 1–5.
[38] M. E. Tipping and C. M. Bishop, "Probabilistic principal component analysis," *J. Roy. Statist. Soc. B*, vol. 61, no. 3, pp. 611–622, 1999.
[39] E. J. Candès, X. Li, Y. Ma, and J. Wright, "Robust principal component analysis?" *J. ACM*, vol. 58, no. 3, p. 11, May 2011.
[40] G. Tang, G. Luo, W. Zhang, C. Yang, and H. Wang, "Underdetermined blind source separation with variational mode decomposition for compound roller bearing fault signals," *Sensors*, vol. 16, no. 6, p. 897, Jun. 2016.
[41] J. Yao, Y. Xiang, S. Li, and S. Wang, "Noise sources identification method of internal combustion engine based on VMD-ICA-CWT," *J. Huazhong Univ. Sci. Technol. Natural Sci. Ed.*, vol. 44, no. 7, pp. 21–24, Jul. 2016.
[42] Z. Ma, X. Liu, J. Zhang, and J. Wang, "Application of VMD-ICA combined method in fault diagnosis of rolling bearings," *J. Vib. Shock*, vol. 36, no. 13, pp. 201–207, Jun. 2017.
[43] W. X. Wu, Z. J. Wang, J. P. Zhang, and J. Y. Wang, "Research of the method of determining K value in VMD based on kurtosis," *J. Mech. Transmiss.*, vol. 42, no. 8, pp. 153–157, Aug. 2018.
[44] X. P. Ren, P. Li, C. G. Wang, and C. Zhang, "Rolling bearing early fault diagnosis based on improved VMD and envelope derivative operator," *J. Vib. Shock*, vol. 37, no. 15, pp. 6–13, Aug. 2018.
[45] Y. Mao, M. Zhao, and J. Lin, "Identification of mechanical compound-fault based on the improved parameter-adaptive variational mode decomposition," *ISA Trans.*, to be published, doi: 10.1016/j.isatra.2018.10.008.
[46] X. Zhang, Q. Miao, H. Zhang, and L. Wang, "A parameter-adaptive VMD method based on grasshopper optimization algorithm to analyze vibration signals from rotating machinery," *Mech. Syst. Signal Process.*, vol. 108, pp. 58–72, Aug. 2018.
[47] E. Moreau, "A generalization of joint-diagonalization criteria for source separation," *IEEE Trans. Signal Process.*, vol. 49, no. 3, pp. 530–541, Mar. 2001.
[48] N. Correa, T. Adalı, and V. D. Calhoun, "Performance of blind source separation algorithms for fMRI analysis using a group ICA method," *Magn. Reson. Imag.*, vol. 25, no. 5, pp. 684–694, Jun. 2007.
[49] M. H. Radfar and R. M. Dansereau, "Single-channel speech separation using soft mask filtering," *IEEE Trans. Audio, Speech, Language Process.*, vol. 15, no. 8, pp. 2299–2310, Nov. 2007.
[50] G. Rilling and P. Flandrin, "One or two frequencies? The empirical mode decomposition answers," *IEEE Trans. Signal Process.*, vol. 56, no. 1, pp. 85–95, Jan. 2008.
[51] M. Craig, "Analytic signals for multivariate data," *Math. Geol.*, vol. 28, no. 3, pp. 315–329, Apr. 1996.
[52] C. C. Celigoj, "An augmented Lagrange multiplier approach to continuum multislip single crystal thermo–elasto–viscoplasticity," *Commun. Numer. Methods Eng.*, vol. 21, no. 7, pp. 357–376, Jul. 2005.
[53] M. A. T. Figueiredo and J. M. Bioucas-Dias, "Restoration of Poissonian images using alternating direction optimization," *IEEE Trans. Image Process.*, vol. 19, no. 12, pp. 3133–3145, Dec. 2010.
[54] B. Hazra, A. Sadhu, A. J. Roffel, P. E. Paquet, and S. Narasimhan, "Underdetermined blind identification of structures by using the modified cross-correlation method," *J. Eng. Mech.*, vol. 138, no. 4, pp. 327–337, Apr. 2012.
[55] X. L. Li, T. Adalı, and M. Anderson, "Joint blind source separation by generalized joint diagonalization of cumulant matrices," *Signal Process.*, vol. 91, no. 10, pp. 2314–2322, Oct. 2010.
[56] M. Kawanabe and F. J. Theis, "Joint low-rank approximation for extracting non-Gaussian subspaces," *Signal Process.*, vol. 87, no. 8, pp. 1890–1903, Aug. 2007.
[57] A. Belouchrani and M. G. Amin, "Blind source separation based on time-frequency signal representations," *IEEE Trans. Signal Process.*, vol. 46, no. 11, pp. 2888–2897, Nov. 1998.
[58] K.-K. Wong, R. D. Murch, and K. B. Letaief, "A joint-channel diagonalization for multiuser MIMO antenna systems," *IEEE Trans. Wireless Commun.*, vol. 2, no. 4, pp. 773–786, Jul. 2003.

YA'NAN ZHANG received the B.S. degree in new energy science and engineering from Hohai University, Nanjing, China, in 2016. He is currently pursuing the M.S. degree in control science and engineering with the Ocean University of China, Tsingtao, China. His research interests include wind energy technology, measurement & control technology, and marine monitoring technology.

SHENGBO QI received the B.S. degree in computer devices engineering from the Huazhong University of Science and Technology, Wuhan, China, in 1994, the M.S. degree in signal and information processing from the Ocean University of China, Tsingtao, China, in 2002, and the Ph.D. degree in mechanical and electronic engineering from Shandong University, Jinan, China, in 2011. From 1994 to 2002, he was a Research Assistant with the Shandong Academy of Sciences. Since 2002, he has been an Associate Professor with the College of Engineering, Ocean University of China. He has authored over 40 articles, and over 20 inventions. His research interests include embedded system, intelligent instruments, and automobile electronics. He is the Executive Director of the Shandong Automation Society and a member of the Council of Shandong Robotics Research Association.

LIN ZHOU received the B.S. degree in automation engineering from the Ocean University of China, Tsingtao, China, in 2002, the M.S. degree in management science from the University of Northampton, Northampton, UK, in 2005, and the Ph.D. degree in port, coastal and offshore engineering from the Ocean University of China, Tsingtao, China, in 2011. He is currently an Associate Professor with the College of Engineering, Ocean University of China. His research interests include offshore wind turbine health monitoring, intelligent information processing, and underwater acoustic positioning technology.